Determination of the High-Pressure Limiting Rate Coefficient and the Enthalpy of Reaction for OH + SO_2

Mark A. Blitz, Kevin J. Hughes, and Michael J. Pilling*

Department of Chemistry, University of Leeds, Leeds, U.K. LS2 9JT

Received: July 15, 2002; In Final Form: December 9, 2002

The kinetics of the association reaction OH + SO_2 have been studied using laser flash photolysis at 248 nm to generate OH radicals and laser-induced fluorescence to monitor their decay under pseudo-first-order conditions, [OH] ≪ [SO_2]. The removal kinetics of OH($v = 1$) + SO_2 have been measured over the temperature range of 295 to 673 K. Master equation calculations were performed to demonstrate that, provided intramolecular vibrational redistribution is fast, OH($v = 1$) + SO_2 is a good approximation for the high-pressure rate coefficient of the OH($v = 0$) + SO_2 + M reaction, giving $k_1^\infty(T) = (2.04 \pm 0.10) \times 10^{-12}$ $(T/300\ \mathrm{K})^{-0.27} \pm 0.11$ cm^3 molecule^{-1} s^{-1}. This temperature dependence of the rate coefficient suggests that the reaction occurs on a barrierless surface. The kinetics of the reaction OH($v = 0$) + SO_2 + M, k_1, were also studied. At room temperature, the kinetic data were in good agreement with literature values. At elevated temperatures, 523 to 603 K, equilibrium behavior was observed between OH + SO_2 and $HOSO_2$. This represents the first direct observation of equilibration, and an analysis of the data, using a Third-Law method, with $\Delta_r S^0_{298} = -142 \pm 10$ J mol^{-1} K^{-1} gives a reaction enthalpy of $\Delta_r H^0_{298} = -113.3 \pm 6$ kJ mol^{-1}, and $\Delta_f H^0_{298}(HOSO_2) = -373 \pm 6$ kJ mol^{-1}. These numerical values are significantly lower than literature values. $k_1^\infty(T)$ has been used to generate a consistent set of parameters to describe $k_1([M], T)$ for OH + SO_2 for use in atmospheric modeling, and $\Delta_r H^0_{298}$ has been used to assess the role of $HOSO_2$ in the oxidation of SO_2 at elevated temperatures.

Introduction

SO_2 is the major form of global anthropogenic sulfur emissions, estimated to be 10^{14} g/yr.[1] The oxidation of SO_2 is believed to be the main route to the formation of H_2SO_4 and consequently plays a significant role in acid rain formation, visibility reduction, and climate modification.[2,3] The first step in the gas-phase oxidation of sulfur dioxide is its reaction with OH:

$$OH + SO_2 + M \rightarrow HOSO_2 + M \qquad (1)$$

Further reactions of $HOSO_2$ with O_2[4] and then of SO_3 with H_2O lead to the formation of H_2SO_4.[5,6] The formation of the $HOSO_2$ adduct has been demonstrated by IR-matrix isolation studies.[7,8] Reaction 1 is pressure-dependent and is in its falloff regime at pressures below atmospheric. Its kinetics over this pressure range have been extensively studied.[9−12] RRKM calculations have been performed, on the basis of these kinetic studies, to obtain the high-pressure limiting rate constant for reaction 1, k_1^∞: Wine et al. recommended a value for k_1^∞ between 260 and 420 K equal to 1.3×10^{-12} $(T/300\ \mathrm{K})^{-0.7}$ cm^3 molecule^{-1} s^{-1}, and Cobos and Troe[13] recommended $k_1^\infty = 2.7 \times 10^{-12}$ exp(−80 K/T) cm^3 molecule^{-1} s^{-1}. These results are the basis for the evaluated temperature-independent value of $k_1^\infty = 2.0 \times 10^{-12}$ cm^3 molecule^{-1} s^{-1} between 200 and 300 K recommended by IUPAC.[14] Recently, however, Fulle et al.[15] have measured k_1 over an extended pressure range of up to 96 atm. The extrapolated k_1^∞ from this study is significantly larger than the IUPAC value, and a positive activation energy of 3 kJ mol^{-1} was observed, which was assigned to a small barrier for the reaction.

The binding energy, $\Delta_r H^0_{298}$, of the $HOSO_2$ adduct was originally estimated by Benson,[16] using a group additivity to be 155 ± 10 kJ mol^{-1}, but further experiments by Gleason and Howard assigned an upper limit of 133 kJ mol^{-1}.[17] The most recent compilation of thermochemical data gives a value of $\Delta_r H^0_{298} = -127$ kJ mol^{-1}.[18] The RRKM fitting of the kinetic data reinforces this assignment for the binding energy,[9,15] but a recent ab initio study by Li and McKee[19] has calculated a considerably lower value for the binding energy of $\Delta_r H^0_{298} = -110$ kJ mol^{-1}.

Although reaction 1 is undoubtedly important in the oxidation of atmospheric SO_2, it has also been proposed in the sulfur-catalyzed recombination of radicals in flames[20] via further reaction of $HOSO_2$:

$$HOSO_2 + H \rightarrow H_2O + SO_2 \qquad (2)$$

This reaction was favored over

$$HOSO_2 + O_2 \rightarrow HO_2 + SO_3 \qquad (3)$$

because Benson's[11] estimate of the binding energy of $HOSO_2$ implies that reaction 3 is endothermic by 25 kJ mol^{-1}. It is now accepted that the binding energy of $HOSO_2$ is considerably less than Benson's original estimate, which affects the relative significance of reactions 2 and 3 in flames.

* Corresponding author. E-mail: m.j.pilling@chem.leeds.ac.uk. Fax: ++44 113 343 6401.

10.1021/jp026524y CCC: $25.00
Published on Web 03/01/2003

In this study, we have investigated the temperature dependence of k_1^∞ to assess the validity of the latest findings of Fulle et al.[15] The value for k_1^∞ was obtained by monitoring the removal of the vibrationally excited hydroxyl radical, OH($v = 1$), in the presence of SO_2:

$$OH(v = 1) + SO_2 \rightarrow \text{products} \qquad (1R)$$

Smith has discussed the validity of using such a method to access the value of the high-pressure limit,[21] and we argue in the Discussion section that it appears that this method does indeed yield the high-pressure limit for OH + SO_2. The binding energy of the $HOSO_2$ adduct was determined by monitoring OH in the presence of SO_2 at elevated temperatures where the reverse reaction

$$HOSO_2 + M \rightarrow OH + SO_2 + M \qquad (-1)$$

competes with the forward reaction, 1, providing a direct measure of the equilibrium constant and hence, via $\Delta_r S^0$, an accurate and reliable measure of the binding energy for $HOSO_2$.

Experimental Section

The laser flash photolysis/laser-induced fluorescence (LIF) system used to perform the experiments is similar to that used in previous studies.[22] Briefly, OH($X\ ^2\Pi$) was generated by the photolysis of $CHBr_3$ (+ SO_2) or H_2O_2 using 50−150 mJ pulses of unfocused 248-nm radiation from an excimer laser (Lambda Physik, LPX100). The OH($v = 0$, 1) radicals were probed via the detection of resonant LIF ($A\ ^2\Sigma^+ \leftarrow X^2\Pi_i$, $v = 0$, $Q_1(1)$, 307.93 nm and $A\ ^2\Sigma^+ \leftarrow X\ ^2\Pi_i$, $v = 1$, $Q_1(1)$, 313.55 nm) using the KDP-doubled output from a Nd:YAG (Spectron, SL803) pumped dye laser (Spectron, SL4000, DCM). The fluorescence passed through an interference filter (Corion, 310 ± 10 nm) and was then detected using a photomultiplier (EMI 9813). The photomultiplier signal was integrated with a boxcar averager (SRS) and digitized before being passed to a personal computer for subsequent data analysis. The delay time between the photolysis laser and probe laser was controlled by the computer, and a kinetic trace consisted of 100 averaged data points, with each point averaged over 6−10 samples. The repetition rate of the lasers was 2 Hz.

Mass flow meters (MKS) were used to control the flow of all reagents, bromoform/He, H_2O_2/He, SO_2, and He, the buffer gas. These gases passed into a mixing manifold before introduction into the reaction cell, based on a six-way cross. Pressures in the cell were measured using capacitance manometers (MKS) and were adjusted by throttling the exit valves on the cell; pressures were adjusted to between 100 and 500 Torr. The total flow was ∼1000 SCCM, ensuring that there was no significant degradation of the sample between laser shots. A metal block around the center of the cell was heated with cartridge heaters, enabling experiments to be performed between 295 and 673 K. The temperature was measured via two thermocouples (type K) probing above and below the reaction zone, ensuring that temperatures were known to better than ±5 K.

Bromoform (Aldrich), H_2O_2 (Aldrich, 35 wt. % solution in water), and SO_2 (Air Products, 99.5%) were degassed and diluted in He, if required, and stored in darkened bulbs. Helium (BOC, CP grade, 99.999%) was used straight from the cylinder.

Results

Removal of OH($v = 1$) with SO_2. SO_2 is photodissociated to form radicals at wavelengths <219 nm,[9] so 248 nm provides the highest-energy excimer laser wavelength that can be used. However, there are no established OH($v = 1$) precursors at this photolysis wavelength; the standard OH precursors HNO_3 and H_2O_2 produce only vibrationally "cold" radicals.[23] In previous work,[24] we observed OH to be a product of the reaction between CH and O_2, so we investigated whether OH($v = 1$) is produced in the reaction between CH and SO_2 by photolyzing the known CH precursor bromoform (0.4 mTorr) in the presence of SO_2. Both OH($v = 0$, 1) were observed, and their rate constant for formation was consistent with 3×10^{-10} molecule^{-1} cm^3 s^{-1}, the previously measured rate constant for the reaction:[25]

$$CH + SO_2 \rightarrow \text{products} \qquad (4)$$

Although we are unable to assign the branching ratio for the OH channel, k_{4a}/k_4, for this reaction

$$CH + SO_2 \rightarrow OH(v = 0, 1) \qquad (4a)$$

previous experiments[24] have shown that an excimer laser generating 150 mJ pulse^{-1} of 248-nm light produces ∼10^{10} molecule cm^{-3} of CH from ∼10^{13} molecule cm^{-3} of bromoform. Therefore, in the present experiments, [OH($v = 0$, 1)] was no greater than 10^{10} molecule cm^{-3}, which is several orders of magnitude less than the added [SO_2], ∼10^{15} to 10^{16} molecule cm^{-3}. Therefore, pseudo-first-order conditions were maintained when monitoring the OH time profiles. In addition, contributions from undetermined radical products from reaction 4 will be unimportant on the experimental time scale. The rate constant k_4 is always at least 100 times faster than k_1 over the conditions investigated, which ensures that, on the experimental time scale of OH removal, OH formation is essentially instantaneous so the OH time profiles are described by a single-exponential equation

$$[OH(v = 1)] = [OH(v = 1)]_0 \exp(-k_{1R}'t) \qquad (5)$$

where $k_{1R}' = k_{1R}[SO_2] + k'$ and k' is the pseudo-first-order rate coefficient for OH removal other than with SO_2. Although it is probable that OH($v = 1$) is initially formed in high rotational states, the total pressures at which the experiment was conducted ensure rapid relaxation, and OH($v = 1$) + SO_2 removal kinetics adhered strictly to eq 5 over the whole temperature range. This excellent single-exponential behavior implies that any additional chemistry that might generate OH($v = 1$) is only occurring to an insignificant extent.

The OH($v = 1$) + SO_2 removal was studied over the temperature range of 295 to 673 K, with the total pressure increased from 100 Torr at room temperature to ∼300 Torr at 673 K. Above this temperature, the bromoform precursor produced species whose fluorescence obscured the OH fluorescence. [SO_2] was varied up to ca. 500 mTorr; above this concentration, fluorescence quenching of OH became a problem. The interference filter used to collect the OH fluorescence reduces the fluorescence from SO_2 to a negligible amount. Figure 1 shows an example of a typical [OH($v = 1$)] trace, while Figure 2 shows an example of a plot of k_{1R}' versus [SO_2]. The slope of such a plot is equal to the bimolecular rate constant for OH($v = 1$) + SO_2. A summary of the results is given in Table 1. The intercept in Figure 2 is the loss of [OH($v = 1$)] from the system via processes other than reaction with SO_2. This loss is mainly due to removal with bromoform, Br_3CH, and its rate is close to the gas kinetic value.[26]

Reaction of OH($v = 0$) with SO_2 at Low Temperatures. The OH($v = 0$) + SO_2 reaction was studied by tuning the probe

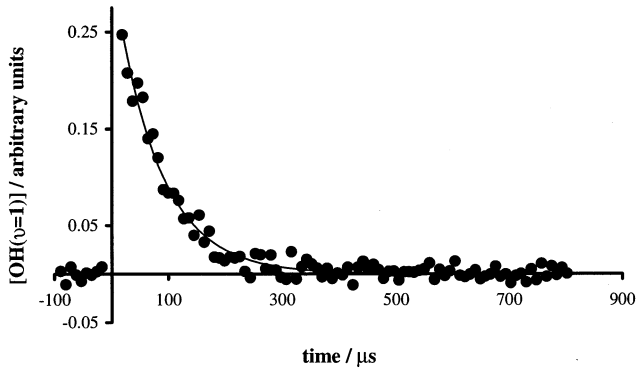

Figure 1. Time profile for OH($v = 1$) in the presence of 174 mTorr of SO_2 at 295 K. The solid line represents the best fit to the data using eq 5.

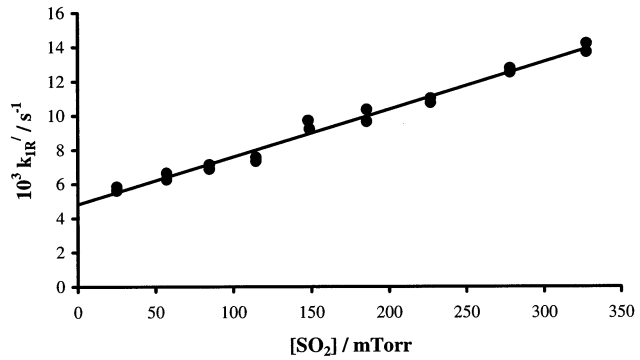

Figure 2. Plot of k_{1R}' versus [SO_2] for [OH($v = 1$)] + SO_2 at 573 K. The slope of this plot yields the bimolecular rate constant given in Table 2.

TABLE 1: Bimolecular Rate Constant, k_{1R}, for the Removal of [OH($v = 1$)] + SO_2[a]

temperature/K	k_{1R}	[SO_2]/mTorr
295	1.97 ± 0.13	55−260
373	1.98 ± 0.10	12−388
473	1.88 ± 0.12	31−522
573	1.65 ± 0.10	25−517
673	1.64 ± 0.17	35−388

[a] Units for k_{1R} are 10^{-12} molecule^{-1} cm^3 s^{-1}, and errors are estimated by propagating the random errors from the data analysis with a 5% general estimate for other sources of uncertainties.

laser to the OH($v = 0$) transition. The data did not strictly adhere to a single exponential but exhibited a long-time tail that is adequately described by a constant background parameter

$$[\mathrm{OH}(v=0)] = [\mathrm{OH}(v=0)]_0 \exp(-k_{\mathrm{obs}}t) + C \qquad (6)$$

where $k_{\mathrm{obs}} = k_1[\mathrm{SO_2}] + k'$ and k' is the pseudo-first-order rate coefficient for OH removal other than with SO_2. Fulle et al.[15] observed such behavior and ascribed the feature to either the reaction of their precursor, ozone, with the adduct

$$\mathrm{HOSO_2} + \mathrm{O_3} \rightarrow \mathrm{HO} + \mathrm{SO_3} + \mathrm{O_2} \qquad (7)$$

or to simultaneous photolysis and probing by the probe laser

$$\mathrm{HOSO_2} + h\nu \rightarrow \mathrm{HO} + \mathrm{SO_2} \qquad (8)$$

The reformation of OH via either reaction 7 or 8 leads to the long-time tail in the decay trace. We favor the explanation provided by a reaction with the precursor, similar to reaction 7, to explain our data because when the precursor was changed to H_2O_2 the data adhered to eq 5. Fitting our [OH($v = 0$)] data to eq 6 enabled k_1 to be determined, but because of this additional complication, the error in k_1 is probably significantly greater than the error in the k_{obs} versus [SO_2] plot. The results for k_1 are given in Table 2, together with the previously measured values of Wine et al.[9]

TABLE 2: Bimolecular Rate Constant, k_1, for the Reaction of [OH($v = 0$)] + SO_2[a]

temperature/K	our data	Wine et al.[9]
295	1.57 ± 0.08 (104 Torr He)	1.03 ± 0.09 (61 Torr He)
		1.21 ± 0.06 (61 Torr Ar)
		1.44 ± 0.01 (123 Torr He)
		1.58 ± 0.13 (123 Torr Ar)
360		0.62 ± 0.03 (61 Torr Ar)
		0.96 ± 0.09 (123 Torr Ar)
373	0.86± 0.09 (103 Torr He)	
420		0.49 ± 0.04 (61 Torr Ar)
		0.72 ± 0.05 (123 Torr Ar)
473	0.98 ± 0.08 (200 Torr He)	

[a] Units for k_1 are 10^{-13} molecule^{-1} cm^3 s^{-1}, and errors represent 2σ.

Observation of Equilibration for OH($v = 0$) + SO_2. At 523 K, the [OH($v = 0$)] data exhibited equilibrium behavior, providing an opportunity to determine the adduct binding energy. However, using bromoform as the precursor requires an independent determination of both k_{-1} and the rate coefficient for reaction with the precursor. These two processes are correlated, and an accurate determination of k_{-1} would be difficult. As only OH($v = 0$) is required, H_2O_2 was used as a clean OH precursor.[23] The photolysis of H_2O_2 in the presence of SO_2 generated [OH($v = 0$)] traces that strictly obeyed eq 5 at temperatures below 473 K. Therefore, it was concluded that at temperatures where equilibrium behavior was observed only k_{-1} was contributing to longer-time OH formation, so the kinetics are well described by reactions 1 and −1 plus a slow loss of OH from the system

$$\mathrm{HO} \rightarrow \mathrm{loss} \qquad (9)$$

which is adequately described by a pseudo-first-order rate constant; the actual mechanism of this loss is speculated upon in the Discussion. From the known 248-nm cross section of H_2O_2[27] at the photolysis energies used, it is readily shown that for initial concentrations of H_2O_2 of 10^{14} molecule cm^{-3} the initial OH concentration produced will be $<10^{12}$ molecule cm^{-3}, so OH + OH can be dismissed as the loss mechanism from the system. Equilibrium OH($v = 0$) kinetic traces were recorded at various [SO_2], up to 1500 mTorr, at a total pressure of ca. 500 Torr; the high total pressure was to counteract reaction 1 moving further into the falloff region at elevated temperatures and thus allowed the observation of equilibrium on a faster time scale, hence allowing a more accurate analysis. An example of such a kinetic trace, exhibiting equilibrium behavior, is show in Figure 3. Data were collected at 523, 543, 563, 583, and 603 K.

Analysis of the Equilibrium Data. The analytic solution for the kinetic scheme that is described by reactions 1, −1, and 9 is a biexponential:

$$[\mathrm{OH}(v=0)] = A \exp(-\lambda_1 t) + B \exp(-\lambda_2 t) \qquad (10)$$

Fitting individual traces to this generic biexponential equation returned consistent parameters. However, the analysis of the system was extended using the technique of global analysis[28] for the simultaneous fitting of multiple [OH($v = 0$)] kinetic traces. A global analysis results in increased model sensitivity

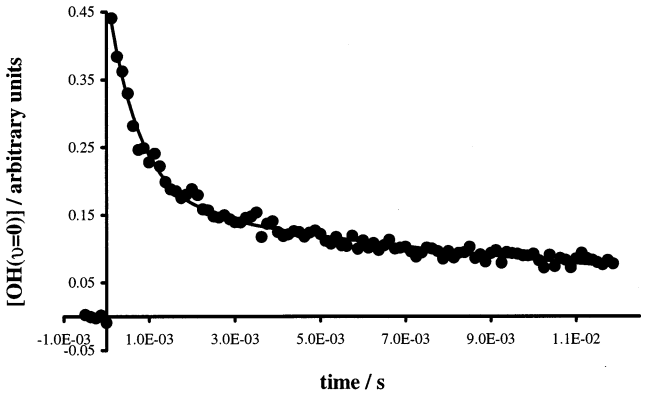

Figure 3. Equilibrium behavior observed in [OH($v = 0$)] + SO_2 at 543 K using 471 mTorr of SO_2. The solid line represents the best fit to the data using eq 10.

and more accurate parameter recovery. The idea behind the simultaneous analysis of multiple kinetic traces is that it exploits relationships between individual traces. Initially, global analysis of the data was performed using the [OH($v = 0$)] kinetic traces at each temperature. This enabled the mechanism of reactions 1, −1, and 9 to be thoroughly tested. The final analysis involved using the kinetic trace from all temperatures.

The coupled ordinary differential equations of schemes 1, −1, and 9 were numerically integrated, generating a trace that was compared with the experimental data, as in single-trace analysis. Each trace has one local parameter $[OH(v = 0)]_0$ and three global rate coefficients k_1, k_{-1}, and k_9. Both global analysis and single-trace analysis employ nonlinear least-squares fitting procedures; therefore, both require the construction of the associated matrices. In global analysis, the global information is allocated to positions within the matrix to which all traces contribute, but local information is allocated to positions to which only an individual trace contributes. The parameter minimization was performed using the Marquardt prescription.[29] The initial analysis of data for individual temperatures described reaction 1 as

$$k_1' = k_1[SO_2] \tag{11}$$

and for all temperatures

$$k_1'(T) = \{k_1(T/500\ \mathrm{K})^{\beta}\}[SO_2] \tag{12}$$

Equation 12 is flexible and is able to accommodate reaction 1 moving further into the falloff region with increased temperature. Through detailed balance, k_{-1} is related to k_1 exactly via the equilibrium constant

$$k_{-1} = \frac{k_1}{K_{eq}} = \frac{k_1}{K_p RT} = \frac{k_1}{RT(\exp(\Delta_r S^0/R)\exp(-\Delta_r H^0/RT))} \tag{13}$$

where K_p is a function of T, $\Delta_r S^0$, and $\Delta_r H^0$. Since $\Delta_r S^0$ can readily be calculated using statistical mechanics to within seven percent, a Third-Law method was employed with $\Delta_r S^0$ fixed at the calculated value, −142 J mol^{-1} K^{-1}, and k_{-1} was adjusted by varying $\Delta_r H^0$. As will be discussed below, both $\Delta_r H^0$ and $\Delta_r S^0$ vary little with temperature. The loss of OH from the system was slow, ∼150 s^{-1}, and was initially assigned to[14]

$$HO + H_2O_2 \rightarrow \text{products} \tag{14}$$

However, it was observed that OH loss (reaction 9) had a dependence on $[SO_2]$, which itself was dependent on the laser photolysis energy. It is known that SO_2 absorption at 248 nm produces excited triplet states, SO_2(T*), that are long-lived;[27] therefore, we suggest that part of the OH loss is via

$$HO + SO_2(T^*) \rightarrow \text{products} \tag{15}$$

Although it is recognized that reaction 15 may lead to nonexponential kinetics, it should be emphasized that the loss of OH from the system is slow compared to the equilibration processes. Therefore, because our measurements focus on the approach to equilibrium, a first-order process can adequately describe reaction 9. In the global analysis, the rate constant for the loss of OH from the system, k_9, was assigned as a local parameter (i.e., each trace had its own OH loss rate constant) that varied somewhat from trace to trace because of differing contributions from reactions 14 and 15. Tables 3 and 4 show the returned global analysis parameters of the system when fitting individual temperatures and all temperatures, respectively. Values for k_9 are not listed. k_9 was typically at least an order of magnitude smaller than the rate constant for the relaxation toward equilibrium, $k_1' + k_{-1}$. An examination of the correlation coefficients in the statistical analysis shows that $\Delta_r H^0$ has only a weak dependence on k_9.

TABLE 3: Global Fitting of the Equilibrium Data[a]

temperature/K	k_1	$\Delta_r H^0_T$/kJ mol	χ^2/pts
523	9.43 ± 0.55	−110.4 ± 0.4	1.202
543	8.22 ± 0.57	−113.3 ± 0.6	1.398
563	4.99 ± 0.49	−112.3 ± 0.4	1.078
583	5.58 ± 0.38	−115.9 ± 0.4	1.159
603	4.79 ± 0.43	−118.6 ± 1.2	1.128

[a] $[SO_2]$ was varied up to 1500 mTorr at a total pressure of ca. 500 Torr. Units for k_1 are 10^{-14} molecule^{-1} cm^3 s^{-1}. Errors represent 2σ.

TABLE 4: Global Parameters from Fitting to All of the Equilibrium Data[a]

number of traces	k_1	β	$\Delta_r H^0_{563}$/kJ mol
55	1.40 ± 0.10	−7.04 ± 0.92	−113.1 ± 0.4

[a] $k_1(T)$ was expressed as $k_1(T/500\ \mathrm{K})^{\beta}$ with units equal to 10^{-13} cm^3 molecule^{-1} s^{-1}. Errors represent 2σ.

Discussion

[OH($v = 0$)] + SO_2. From Table 2, it can be seen that there is reasonable agreement between our measured rate constants for reaction 1 and those of Wine et al.[9] As discussed in the results section, the OH($v = 0$) profiles with a Br_3CH precursor exhibited a long-time tail and the data were fitted to an exponential plus background, eq 6. Uncertainty in the origin of the tail means systematic errors in k_1 could significantly add to the errors quoted in Table 1, which include random errors from fitting the data and contributions from other experimental factors, e.g. concentration measurements. It is concluded that, within error, our results are in agreement with those of Wine et al.[9]

[OH($v = 1$)] + SO_2; High-Pressure Limit. Table 1 shows the rate constants for the removal of OH($v = 1$) with SO_2, k_{1R}. The OH($v = 1$) time profiles adhered strictly to single-exponential behavior. The errors in the rate constants in Table 1 are reasonably estimated by propagating the random errors from the data analysis with a 5% general estimate for other sources of uncertainties. The data in Table 1 were fitted to the function

$$k_1^{\infty}(T) = A(T/300\ \mathrm{K})^{-n} \tag{16}$$

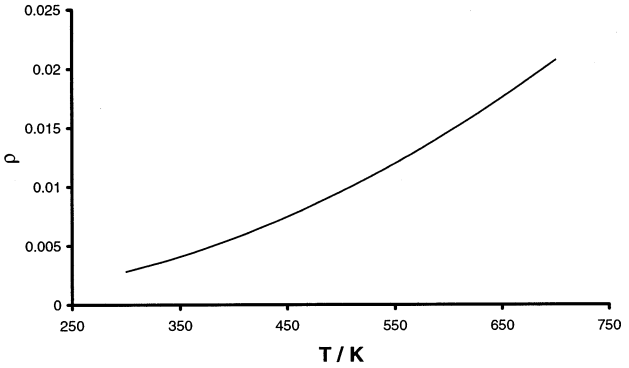

Figure 4. Plot of ρ vs T. This plot shows that the even at our highest experimental temperature the formation of OH($v = 1$) from the dissociation of the adduct is ca. 2%.

giving $A = (2.04 \pm 0.10) \times 10^{-12}$ molecule^{-1} cm^3 s^{-1} and $n = 0.27 \pm 0.11$ (errors are $\pm 2\sigma$). The data were weighted in the fitting using the error associated with each rate constant.

The removal of vibrational energy from a diatomic via a chemically inert collision partner can occur via transfer of the vibrational energy into the translational, rotational, and vibrational energy of the collision partner, but all of these processes are comparatively slow for nonresonant transfer involving nonhydrides.[30] The vibrational frequencies for OH and SO_2 are 3570 and 1362, 1157, and 517 cm^{-1}, respectively, so that V−V bimolecular transfer is far from resonant. The assignment of the rate coefficient for the removal of OH($v = 1$) with SO_2 to the high-pressure limiting rate constant for reaction 1, k_1^∞, assumes that energy transfer via mechanisms other than the formation of $HOSO_2$ is slow. If this assumption is invalid, then the measurement provides an upper limit for k_1^∞. Smith and co-workers[31] have extensively used the rate coefficients for the reaction of vibrationally excited radicals with species that form association adducts as a way of determining the high-pressure limiting rate coefficient, k^∞.

It is also assumed that rapid intramoleuclar vibrational energy redistribution ensures that the dissociation of the adduct leads to the formation of the radical in its ground vibrational state. If OH($v = 1$) is regenerated at a significant rate, then k_1^∞ will be underestimated. The extent of underestimation will be greatest at the lowest pressure because increasing [M] will lead to more stabilization of the adduct and a decrease in the rate of forming OH($v = 1$). The worst-case scenario is at the limit of zero pressure; at this limit, the energy-grained master equation (ME) for the system is

$$\frac{dn_i}{dt} = g_i - (k_i^0 + k_i^1)n_i \tag{17}$$

where n_i is the population of the ith energy grain of $HOSO_2$, g_i is the rate of formation from OH($v = 1$) + SO_2, and k_i^0 and k_i^1 are the microcanonical rate coefficients for dissociation from grain i to form OH($v = 0$) and OH($v = 1$), respectively. Since the grains are not collisionally coupled, the ME is readily solved in the steady state to give

$$n_i = \frac{g_i}{k_i^0 + k_i^1} \tag{18}$$

where

$$g_i = \frac{R^\infty k_i^1 N_i \exp(-\beta E_i)}{\Sigma k_i^1 N_i \exp(-\beta E_i)} \tag{19}$$

N_i is the number of rovibrational states in grain i, $\beta = 1/k_B T$, and $R^\infty = k_1^\infty[\mathrm{OH}(v = 1)][SO_2]$. Note that the assumption has been made that the high-pressure rate coefficients are identical for $v = 0$ and 1.

The ratio, ρ, of the rates of formation of $v = 1$ and 0 on the dissociation of the adduct at zero pressure is

$$\rho = \frac{\sum_{E_{v=1}}^{\infty} k_i^1 n_i}{\sum_{E_{v=1}}^{\infty} k_i^0 n_i} = \frac{\sum_{E_{v=1}}^{\infty} \frac{(k_i^1)^2}{k_i^0 + k_i^1} N_i \exp(-\beta E_i)}{\sum_{E_{v=1}}^{\infty} \frac{k_i^0 k_i^1}{k_i^0 + k_i^1} N_i \exp(-\beta E_i)} \tag{20}$$

where $E_{v=1}$ is the threshold energy for dissociation to form $v = 1$, hence for the formation of $HOSO_2$ from OH($v = 1$).

k_i^0 and k_i^1 were calculated from $k_1^\infty(T)$ using an inverse Laplace transformation.[32] Both our value of $k_1(T) = (2.04 \pm 0.10) \times 10^{-12}$ $(T/300\ \mathrm{K})^{-0.27\pm0.11}$ cm^3 molecule^{-1} s^{-1} and the value of Fulle et al.[15] were used as the expression for $k_1^\infty(T)$ in the inverse Laplace transformation; ρ was found to be insensitive to the choice of $k_1^\infty(T)$. Figure 4 shows a plot of ρ versus T over the experimental temperature range. As expected, ρ increases with T but even at 700 K is only 0.02, well within experimental error. At experimental pressures of 100−300 Torr, the production of OH($v = 1$) will be reduced still further, and we may conclude that its regeneration by the dissociation of $HOSO_2$ following formation from OH($v = 1$) + SO_2 is not significant in our experiments. This calculation also implies that OH($v = 2$) + SO_2 predominantly produces OH($v = 0$), hence OH($v = 2$) will not interfere with the OH($v = 1$) + SO_2 removal kinetics.

This analysis implicitly assumes that a statistical treatment of association/dissociation is appropriate. If intramoleuclar vibrational redistribution (IVR) were incomplete in the adduct formed from OH($v = 1$), then some regeneration of vibrationally excited OH might occur, reducing the measured rate constant. Smith[21] has discussed the likelihood of IVR being incomplete before dissociation, and it may be gauged by considering the lifetime of the association complex, $HOSO_2$ in our case. A reasonable estimate of the lifetime of the complex, τ_{HOSO_2}, is given by[21]

$$\tau_{HOSO_2} = \frac{k_1^0}{\beta_c Z^0 k_1^\infty} \tag{21}$$

where β_c is a parameter that allows for the failure of the strong collision hypothesis[33] and Z^0 is the gas kinetic frequency for collision between OH and SO_2. Values for $k_1^0(T)$ and $k_1^\infty(T)$ are given later in the Application to Atmospheric Chemistry section of the Discussion. $\beta_c = 0.2$ is a reasonable estimate for N_2, and $Z^0 \approx 3 \times 10^{-10}$ cm^3 molecule^{-1} s^{-1}. Therefore, it may be estimated that τ_{HOSO_2}, the average lifetime of the energized $HOSO_2$, varies from 3 ns at 300 K to 0.1 ns at 700 K. These lifetimes represent thousands of periods of vibration for the complex, which make it extremely unlikely that IVR is

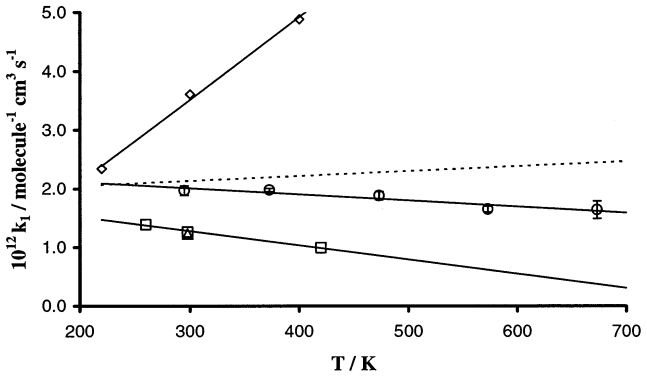

Figure 5. High-pressure limiting rate constants k_1^∞: ○, this work; ◇, Fulle et al.;[15] □, Wine et al.;[9] △, Paraskevopoulos et al.[10] and - - -, Cobos et al.[38] The error bars in our data refer only to the statistical errors returned from the bimolecular plots, 2σ.

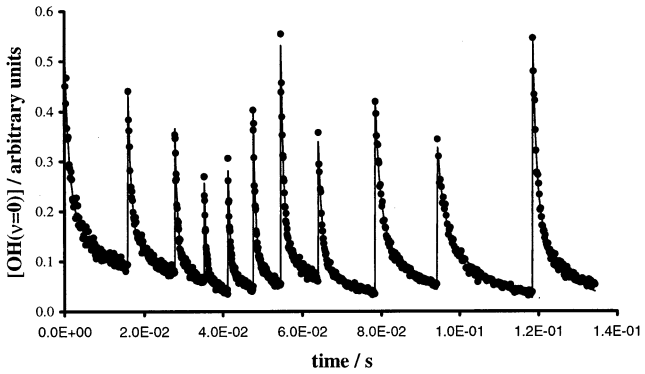

Figure 6. Global analysis fit to [OH($v = 0$)] + SO_2 at 543 K. The 11 separately determined experimental traces at this temperature are displayed by aligning the traces next to one another in time. ●, Experimental data; —, fit to the data. The end of one trace and the beginning of the next is shown by the sharp rise in the solid line.

incomplete. Incomplete IVR could lead to the regeneration of OH(v=1) (i.e., to ρ values significantly greater than zero) and to an underestimate of $k_1^\infty(T)$. The foregoing discussion suggests that this is improbable unless IVR in $HOSO_2$ behaves pathologically.

The high-pressure rate constant for reaction 1, k_1^∞, determined from previous studies[9,10,13,15] has been determined by extrapolations of experimental data using RRKM rate theory.[33,34] Fulle et al., by contrast, approached the limit more closely using very high pressure.[15] These values for k_1^∞ are plotted in Figure 5, together with our data from Table 1. From Figure 5 at 295 K, it can be seen that our data are in good agreement with those of Cobos et al.[13] and are ~35% larger than those of Wine et al. and Paraskevopoulos et al.;[9,10] these studies were the basis for the IUPAC recommendation of 2.0×10^{-12} cm^3 molecule^{-1} s^{-1}, independent of temperature between 200 and 300 K.[14] However, our value at 295 K is about a factor of 2 smaller than that of Fulle et al.[15] From Figure 5, it can be seen that our values for k_1^∞ show a small negative temperature dependence, in agreement with the data from Wine et al.,[9] and although Cobos et al.[13] derived a small positive temperature dependence, the overall discrepancy is not too large; these investigations together suggest a barrierless potential energy surface. However, this weak dependence in $k_1^\infty(T)$ is in contrast to the larger, positive dependence found in the study by Fulle et al.,[15] where it was argued that this observation together with the magnitude of k_1^∞ provides evidence for a small barrier of ~3 kJ mol^{-1} along the surface of reaction 1. Although the magnitude of k_1^∞ is low for a reaction on a barrierless surface, there are good examples of low A factors for reactions where significant electronic rearrangement occurs. For example, $CH_3 + O_2$ has a high-pressure limiting rate coefficient at 300 K of 1.8×10^{-12} cm^3 molecule^{-1} s^{-1} with a slight positive T dependence and provides an interesting comparator.[18]

OH + SO_2 ⇌ $OHSO_2$; Binding Energy of $HOSO_2$. The entropy of reaction 1 was fixed in the global analysis because it can readily be calculated to within 7% and hence leads to a more accurate determination of the enthalpy of reaction 1, the binding enthalpy of $HOSO_2$. From the study by Nagase et al.,[8] a combination of matrix isolation and ab initio calculations was used to characterize the $HOSO_2$ radical. We assigned these constants in this paper, using the experimental values when possible, to calculate the entropy of $HOSO_2$. These molecular parameters together with the parameters for OH and SO_2 are listed in the Appendix. The entropy change calculated for reaction 1 is $\Delta_r S^0_{298} = -142$ J mol^{-1} K^{-1}, which is in good agreement with the value of -140 J mol^{-1} K^{-1} calculated by ab initio methods by Li and McKee.[19] It was found that the calculated entropy change is essentially unchanged when converted to 563 K, the average temperature of the experiments. The global analysis parameters that were returned at each temperature are given in Table 3. Each kinetic trace was assigned its own OH-loss rate constant, reaction 9; these are not listed in Table 3 but were typically ca. 150 s^{-1}. An example of the quality of the fit from the global analysis is shown in Figure 6. From Table 3, it can be seen that the middle temperatures yield a consistent value for $\Delta_r H^0_T$, the enthalpy change for reaction 1. There are, however, larger differences at the two extreme temperatures. This is not too surprising because at the temperature extremes the equilibrium behavior is difficult to discern: at low temperatures, there is almost no reverse reaction, and at high temperatures, the reverse reaction is rapid. To minimize these problems, the global analysis was extended to fit the data at all temperatures simultaneously, and the results are shown in Table 4. This fit gave χ^2/pts = 1.410, which represents only a slight loss in "goodness of fit" compared to the individual temperature analysis. The returned value for $\Delta_r H^0_{563} = -113.1 \pm 0.4$ kJ mol^{-1} is close to the average from the individual temperature analysis. To estimate the uncertainty in $\Delta_r H^0_T$, the global analysis was repeated with $\Delta_r S^0$ varied over a range of values using $\Delta_r S^0_{298} = -142 \pm 10$ J mol^{-1} K^{-1} to represent the 95% confidence level; all other uncertainties are smaller and should be contained within this range. The global analysis gives $\Delta_r H^0_{563} = -113.1 \pm 6$ kJ mol^{-1}, in excellent agreement with the ab initio value of $\Delta_r H^0_{563} = -110$ kJ mol^{-1} that was recently calculated by Li and McKee.[19] Since the early value of Benson[16] of 155 kJ mol^{-1}, estimates of the binding energy of $HOSO_2$ have decreased; Gleason and Howard placed an upper limit of 138 kJ mol^{-1} in their study on reaction 3, and IUPAC in 1997[18] recommended a value of 128 kJ mol^{-1} from an evaluation of the literature. However, the present measurements represent the first direct observation of equilibration in the reaction between HO and SO_2 and provide the most reliable and accurate value for the binding energy of the $HOSO_2$ radical. The conversion of the enthalpy to 298 K produces almost no change in the value and gives $\Delta_r H^0_{298} = -113.3 \pm 6$ kJ mol^{-1}. Taking $\Delta_f H^0_{298}$(OH) = 37.2 kJ mol^{-1} [35] and $\Delta_f H^0_{298}$(SO2) = -296.8 kJ mol^{-1} [36] gives $\Delta_f H^0_{298}(HOSO_2) = -373 \pm 6$ kJ mol^{-1}

Application to Atmospheric Chemistry. Atmospheric models require parametrized forms of rate constants for pressure-dependent reactions. The OH + SO_2 reaction is a bimolecular addition reaction, and for atmospheric modeling, its rate constant

is generally parametrized by the following expression:[14]

$$k_1([M], T) = k_1^{\infty}(T)\, F_{LH}([M], T)\, F \tag{22}$$

F_{LH} is the Lindemann−Hinshelwood expression, and F is the broadening factor given by

$$\log F = \frac{\log F_c}{1 + [\log(k_1^0/k_1^{\infty})]^2} \tag{23}$$

where F_c characterizes the broadening. The k_1 pressure-dependence measurements in this study reinforce the values previously determined by Wine et al.[9] In addition, this study has also determined $k_1^{\infty}(T)$; therefore, it is now possible to combine the literature data with $k_1^{\infty}(T)$ to obtain a better set of fitting parameters. From above, the temperature dependence for k_1^{∞} is given by

$$k_1^{\infty}(T) = 2.04 \times 10^{-12}(T/300\ \mathrm{K})^{-0.27}\ \mathrm{cm^3\ molecule^{-1}\ s^{-1}} \tag{16}$$

The unknown parameters in eq 22 are $k_1^0(T)$ and F_c. $k_1^0(T)$ is described by

$$k_1^0(T) = k_1^0(T/300\ \mathrm{K})^{-m} \tag{24}$$

and F_c is described by

$$F_c = \exp(-T/T^*) \tag{25}$$

where T^* is the fitting parameter. For atmospheric modeling purposes, the data used in the fitting should be for M = N_2 or air (O_2 is typically indistinguishable from N_2 as a third body). The falloff data set with M = N_2 is limited to room temperature, but there is a much more extensive falloff data set for M = Ar. To circumvent this problem, we have calculated the temperature dependence in k_1^0 (i.e., m in eq 24) using a master equation approach. This calculation of the temperature dependence is probably more reliable than the extrapolated experimental value. First, k_1^0 for Ar at room temperature was matched to the experimental value by adjusting $\langle\Delta E\rangle_{down}$ (= 160 $\mathrm{cm^{-1}}$). Then, k_1^0 for Ar was generated over the temperature range of 260−360 K, with good agreement between the calculated and experimental temperature dependence for k_1^0. Then, $\langle\Delta E\rangle_{down}$ was adjusted to match k_1^0 for N_2 at room temperature,[9] giving $\langle\Delta E\rangle_{down}$ = 313 $\mathrm{cm^{-1}}$. Finally, k_1^0 for N_2 was generated over the temperature range of 250−370 K, which was then fitted to eq 24 to yield m = 4.09.

The literature data for OH + SO_2 + M (= N_2) of Wine et al.[9] and Paraskevopoulos et al.[10] were fitted to eq 24; $k_1^0(T)$ and $k_1^{\infty}(T)$ were fixed to the expressions determined above. The following parameters were obtained (errors represent $\pm 1\sigma$):

$$F_c = \exp(-T/(412 \pm 30))$$

$$k_1^0(T) = (3.44 \pm 0.21) \times 10^{-31}(T/300\ \mathrm{K})^{-4.09}\ \mathrm{cm^6\ molecule^{-2}\ s^{-1}}$$

$$k_1^{\infty}(T) = (2.04 \pm 0.10) \times 10^{-12}(T/300\ \mathrm{K})^{-0.27\pm0.11}\ \mathrm{cm^3\ molecule^{-1}\ s^{-1}}$$

These fitting parameters are comparable with those of the IUPAC evaluation[14]

$$k_1^0(T) = (4.0 \pm 1.0) \times 10^{-31}(T/300\ \mathrm{K})^{-3.3\pm1.1}\ \mathrm{cm^6\ molecule^{-2}\ s^{-1}}$$

$$k_1^{\infty} = 2 \times 10^{-12}\ \mathrm{cm^3\ molecule^{-1}\ s^{-1}}$$

over T = 200−300 K and F_c = 0.45 near 300 K. Our derived fitting parameters represent an improvement over their accuracy because our measurements on OH(v = 1) + SO_2 have allowed $k_1^{\infty}(T)$ to be reliably fixed. As noted above, there is a discrepancy between our data for $k_1^{\infty}(T)$ and that of Fulle et al.[15] Since the fitting parameters are strongly correlated with $k_1^{\infty}(T)$, their recommended fitting parameters will reflect this inconsistency.

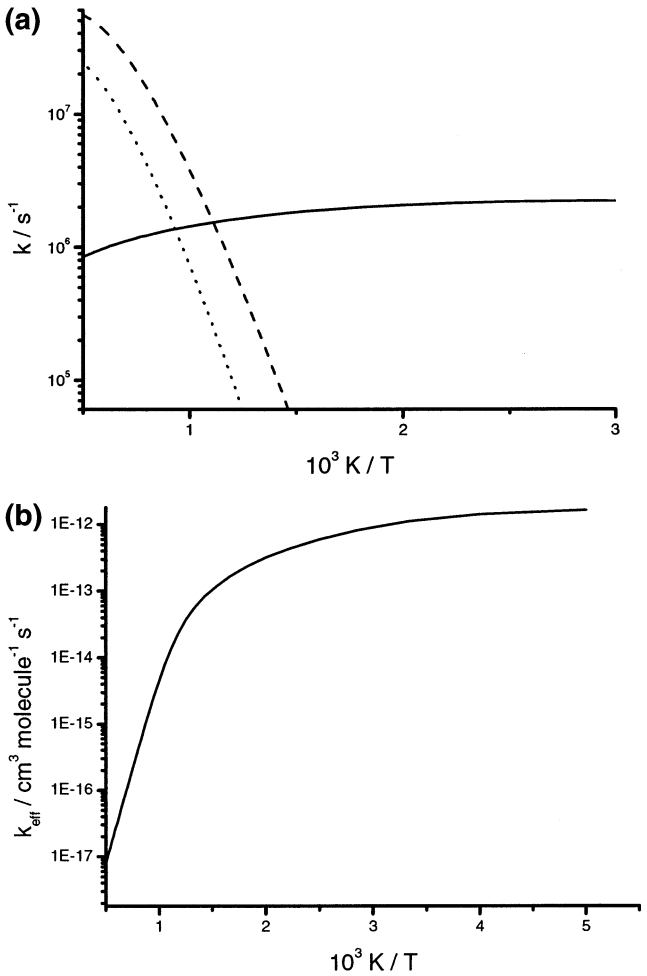

Figure 7. (a) Arrhenius plots for k_{-1} and for $k_3[O_2]$ (—) vs $1/T$. k_{-1} was calculated from $k_1([M], T)$ coupled with either the thermodynamic data derived above, $\Delta_r H^0_{298}$ = −113.3 kJ $\mathrm{mol^{-1}}$, (- - -) or the previously recommended value, $\Delta_r H^0_{298}$ = −127 kJ $\mathrm{mol^{-1}}$ [18] (···). (b) Arrhenius plot for k_{eff}. Note the dramatic fall in k_{eff} after the onset of equilibrium in OH + SO_2 and $HOSO_2$.

Implications for the Oxidation of SO_2 in Combustion Systems. As previously noted, the primary mechanism for the oxidation of SO_2 proceeds through reactions 1 and 3, viz., the formation of $HOSO_2$ followed by its reaction with O_2. If a steady state is assumed for the adduct, $HOSO_2$, then the rate of formation of SO_3 is $k_{eff}[OH][SO_2]$, where

$$k_{eff} = \frac{k_1 k_3[O_2]}{k_{-1} + k_3[O_2]}$$

Figure 7a shows Arrhenius plots for k_{-1} at 1 bar total pressure

and for $k_3[O_2]$,[12,17] where $[O_2] = 0.2$ bar; k_{-1} was calculated from eq 22, where $k_1^\infty(T) = 2.04 \times 10^{-12}(T/300\ \mathrm{K})^{-0.27}$ cm^3 molecule^{-1} s^{-1}, $k_1^0(T) = 3.44 \times 10^{-31}(T/300\ \mathrm{K})^{-4.09}$ cm^6 molecule^{-2} s^{-1}, and F_c was estimated to be 0.6, coupled with either the thermodynamic data derived above, $\Delta_rH^0_{298} = -113.3$ kJ mol^{-1}, or the previously recommended value, $\Delta_rH^0_{298} = -127$ kJ mol^{-1}.[18] The first-order rate coefficients k_{-1} and $k_3[O_2]$ become equal at either 899 or 1173 K for our $\Delta_rH^0_{298}$ and the literature $\Delta_rH^0_{298}$, respectively. Further increases above these temperatures significantly reduce the effectiveness of this oxidation route, as demonstrated in Figure 7b, which shows an Arrhenius plot for k_{eff}, using our value for $\Delta_rH^0_{298}$. In aircraft engines, the combustion of sulfur-containing fuels produces SO_2, and at reduced postcombustion temperatures, further oxidation to SO_3 may occur via the above mechanism; SO_3 further reacts with H_2O to form sulfuric acid, which plays an important role as a sulfate aerosol precursor. Model simulations of aircraft engines using sulfur-containing fuels have highlighted the importance of the OH + SO_2 reaction in explaining the SO_3 and H_2SO_4 concentrations,[37] this reaction being more important than O + SO_2. However, from Figure 7a, it can be seen that our experimental value for $\Delta_rH^0_{298}$ reduces the effectiveness of this oxidation route at higher temperatures, hence future modeling studies might need to reexamine the role of the OH + SO_2 reaction.

Conclusions

The removal between OH($v = 1$) + SO_2 has been studied as a function of temperature for the first time to provide a reliable estimate of the high-pressure limiting rate coefficient for reaction 1, k_1^∞. The slight negative T dependence of $k_1^\infty(T)$ implies that reaction 1 occurs on a barrierless surface, in agreement with Wine et al.,[9] but is in conflict with Fulle et al.,[15] who observed a higher rate coefficient over our experimental range and a positive temperature dependence. At elevated temperatures, equilibrium behavior was observed for the first time between OH($v = 0$) + SO_2 and $HOSO_2$, and these data yield $\Delta_rH^0_{298} = -113.3 \pm 6$ kJ mol^{-1}, which is significantly less than previous literature estimates but in agreement with a recent ab initio value. The impact of the results in this study has been assessed in the context of atmospheric and combustion chemistry.

Acknowledgment. We thank EPSRC for research funding and Professors Ian W.M. Smith and Reinhard Zellner for helpful discussions. K.J.H. was financially supported by the EC GROWTH Program, Research Project PARTEMIS, Measurement and Prediction of Emissions of Aerosols and Gaseous Precursors from Gas Turbine Engines, contract G4RD-CT2000-00207.

Appendix

The following molecular parameters have been used to calculate the entropy change in reaction 1.

HO:	$v/\mathrm{cm}^{-1} = 3570$[36]
	$B(\mathrm{cm}^{-1}) = 18.87$[36]
	$Q_{\mathrm{el}} = 2 + 2\exp(-139.7\ \mathrm{cm}^{-1}\ hc/kT)$[36]
SO_2:	$v/\mathrm{cm}^{-1} = 1362, 1151, 517$[36]
	$B(\mathrm{cm}^{-1}) = 0.5792$[36]
	$Q_{\mathrm{el}} = 1$
$HOSO_2$:	$v/\mathrm{cm}^{-1} = 3528, 1309, 1181, 1097, 760, 544, 491, 437, 252$[8]
	$B(\mathrm{cm}^{-1}) = 0.2627$
	$Q_{\mathrm{el}} = 2$

References and Notes

(1) Singh, H. B.; Chen, Y.; Gregory, G. L.; Sachse, G. W.; Talbot, R.; Blake, D. R.; Kondo, Y.; Bradshaw, J. D.; Heikes, B.; Thornton, D. *Geophys. Res. Lett.* **1997**, *24*, 127.

(2) Calvert, J. G.; Galloway, J. N.; Hales, J. M.; Hidy, G. M.; Jacobsen, J. S.; Lazrus, A.; Miller, J. M.; Mohnen, V. *Acid Deposition: Atmospheric Process in Eastern North America*; Committee on Atmospheric Transport and Chemical Transformation in Acid Precipitation, Environmental Studies Board, National Research Council; National Academy Press: Washington, DC, 1983.

(3) Calvert, J. G.; Lazrus, A.; Kok, G. L.; Heikes, B. G.; Walega, J. G.; Lind, J.; Cantrell, C. A. *Nature (London)* **1985**, *317*, 27.

(4) Stockwell, W. R.; Calvert, J. G. *Atmos. Environ.* **1983**, *17*, 2231.

(5) Lovejoy, E. R.; Hanson, D. R.; Huey, L. G. *J. Phys. Chem.* **1996**, *100*, 19911.

(6) Reiner, T.; Arnold, F. *J. Chem. Phys.* **1994**, *101*, 7399.

(7) Hashimoto, S.; Inoue, G.; Akimoto, H. *Chem. Phys. Lett.* **1984**, *107*, 198.

(8) Nagase, S.; Akimoto, H. *J. Phys. Chem.* **1988**, *92*, 641.

(9) Wine, P. H.; Thompson, R. J.; Ravishankara, A. R.; Semmes, D. H.; Gump, C. A.; Torabi, A.; Nicovich, J. M. *J. Phys. Chem.* **1984**, *88*, 2095.

(10) Paraskevopoulos, G.; Singleton, D. L.; Irwin, R. S. *Chem. Phys. Lett.* **1983**, *100*, 83.

(11) Lee, Y. Y.; Kao, W. C.; Lee, Y. P. *J. Phys. Chem.* **1990**, *94*, 4535.

(12) Martin, D.; Jourdain, J. L.; Lebras, G. *J. Phys. Chem.* **1986**, *90*, 4143.

(13) Cobos, C. J.; Troe, J. *J. Chem. Phys.* **1985**, *83*, 1010.

(14) Atkinson, R.; Baulch, D. L.; Cox, R. A.; Hampson, R. F.; Kerr, J. A.; Rossi, M. J.; Troe, J. *J. Phys. Chem. Ref. Data* **1997**, *26*, 1329.

(15) Fulle, D.; Hamann, H. F.; Hippler, H. *PCCP Phys. Chem. Chem. Phys.* **1999**, *1*, 2695.

(16) Benson, S. W. *Chem. Rev.* **1978**, *78*, 23.

(17) Gleason, J. F.; Howard, C. J. *J. Phys. Chem.* **1988**, *92*, 3414.

(18) Atkinson, R.; Baulch, D. L.; Cox, R. A.; Hampson, R. F.; Kerr, J. A.; Rossi, M. J.; Troe, J. *J. Phys. Chem. Ref. Data* **1997**, *26*, 521.

(19) Li, W. K.; McKee, M. L. *J. Phys. Chem. A* **1997**, *101*, 9778.

(20) Wheeler, R. J. *J. Phys. Chem.* **1968**, *72*, 3359.

(21) Smith, I. W. M. *J. Chem. Soc., Faraday Trans.* **1997**, *93*, 3741.

(22) Blitz, M. A.; Beasley, M. S.; Pilling, M. J.; Robertson, S. H. *PCCP Phys. Chem. Chem. Phys.* **2000**, *2*, 805.

(23) Schiffman, A.; Nelson, D. D.; Nesbitt, D. J. *J. Chem. Phys.* **1993**, *98*, 6935.

(24) Blitz, M. A.; Johnson, D. G.; Pesa, M.; Pilling, M. J.; Robertson, S. H.; Seakins, P. W. *J. Chem. Soc., Faraday Trans.* **1997**, *93*, 1473.

(25) Zabarnick, S.; Fleming, J. W.; Lin, M. C. *Int. J. Chem. Kinet.* **1989**, *21*, 765.

(26) Johnson, D. G. Ph.D. Thesis, University of Leeds, Leeds, U.K., 1999.

(27) Okabe, H. *Photochemistry of Small Molecules*; Wiley & Sons: New York, 1978.

(28) Knutson, J. R.; Beechem, J. M.; Brand, L. *Chem. Phys. Lett.* **1983**, *102*, 501.

(29) Marquardt, D. W. *J. Soc. Ind. Appl. Math.* **1963**, *11*, 1431.

(30) Lambert, J. D. *Vibrational and Rotational Relaxation in Gases*; Clarendon Press: Oxford, 1977.

(31) Brownsword, R. A.; Canosa, A.; Rowe, B. R.; Sims, I. R.; Smith, I. W. M.; Stewart, D. W. A.; Symonds, A. C.; Travers, D. *J. Chem. Phys.* **1997**, *106*, 7662.

(32) Davies, J. W.; Green, N. J. B.; Pilling, M. J. *Chem. Phys. Lett.* **1986**, *126*, 373.

(33) Holbrook, K. A.; Pilling, M. J.; Robertson, S. H. *Unimolecular Reactions*; Wiley & Sons: New York, 1996.

(34) Gilbert, R. G.; Smith, S. C. *Theory of Unimolecular and Recombination Reactions*; Blackwell: Oxford, U.K., 1990.

(35) Ruscic, B.; Wagner, A. F.; Harding, L. B.; Asher, R. L.; Feller, D.; Dixon, D. A.; Peterson, K. A.; Song, Y.; Qian, X. M.; Ng, C. Y.; Liu, J. B.; Chen, W. W. *J. Phys. Chem. A* **2002**, *106*, 2727.

(36) Chase, M. W.; Davies, C. A.; Downey, J. R.; Frurip, D. J.; McDonald, R. A.; Syverud, A. N. *J. Phys. Chem. Ref. Data* **1985**, *14*, 1.

(37) Tremmel, H. G.; Schumann, U. *Aerosp. Sci. Technol.* **1999**, *3*, 417.

(38) Cobos, C. J.; Hippler, H.; Troe, J. *J. Phys. Chem.* **1985**, *89*, 1778.